Theoretical energy distributions around threshold from coherent pion production

P. A. Deutchman
Physics Department, University of Idaho, Moscow, Idaho 83843
(Received 30 June 1992)

Detailed energy distributions have been calculated for exclusive π^0 production in C+C collisions below and above threshold. The quantum-coherent, microscopic, many-body formalism used previously has been extended to include the ρ-exchange as well as the π-exchange interaction modified to produce nucleon isobars in the intermediate nuclear states. Analytic solutions to the Δ-hole and particle-hole coefficients using the degenerate, schematic-model approximation are used where collective-coherent, spin-isospin giant resonances are assumed for the nuclear excited states. The nuclear form factors that depend on these coefficients are solved analytically and become sums of degenerate Δ-hole and particle-hole states for given multipole angular momentum values of the excited nuclei. Also, in this approach, the overall amplitudes and differential cross sections for π^0 production in either nucleus have been formally solved and the first numerical results of the pion, kinetic-energy distributions are presented.

PACS number(s): 25.70.−z, 24.10.Cn, 24.30.Cz

A recent experiment on $^{12}C[^{12}C,^{12}C(1^+,T=1;\ 15.1\ \text{MeV})]X\pi^0$ at 95 MeV/nucleon has been reported by Erazmus *et al.* [1] that strongly suggests the existence of a coherent subthreshold pion-production process. Even though there has been no completely exclusive data taken, this more exclusive experiment provides new excitement and renewed hope to those searching for a quantum-mechanical, coherent signature that may occur in pion production experiments in the subthreshold or near-threshold regions. A number of authors have proposed various collective or coherent models as playing a role in the interpretation of pion production near threshold [2–8] and it is pointed out by Braun-Munzinger and Stachel [9] that observed cross sections cannot yet be fully understood, which implies a need for the inclusion of a coherent model. Having just completed the codes for the formalism that will be outlined below, numerical results of the energy distributions for π^0 production below and above threshold (~290 MeV/nucleon) will be presented. Because of the preliminary nature of this experiment and the sense of immediacy, the results of the theory at its present stage of development will be suggestive of the approximate magnitudes, shapes, and trends of coherent pion distributions. It is hoped that these results can serve as a useful indicator of results that might be obtained in future, more detailed experiments.

The formal solutions of the second-order amplitude in the Born approximation for π^0 production from the collision of equal-mass nuclei where Δ-hole states are created in the intermediate nuclei have been previously described [8]. In that work, the nuclear form factors [see Eqs. (18) and (23)] were solved in terms of the unknown Δ-hole coefficients $x_{\Delta h}$ and particle-hole coefficients $x_{\rm ph}$. In this paper, the analytic solutions of these coefficients are presented, using the degenerate schematic model [10]. The generalized angular-momentum coupled operator that generates all collective giant resonance states of total angular momentum multipole J, orbital angular momentum multipole L, transition-spin $\mathbf{S}$, transition-isospin T^{T_z} is given by

$$O=\sum_{JLMT_z}[r^L\mathbf{Y}_L(\hat{\mathbf{r}})\times\mathbf{S}]^M_J T^{T_z}\ . \tag{1}$$

For example, the target Δ-hole coefficient in nuclear excited state α generated by (1) becomes

$$x^{\alpha}_{\Delta h}(T)=N^{L_T}_{\alpha(T)}O^{J_TL_T}_{\Delta h}\ , \tag{2}$$

where the normalization factor $N^{L_T}_{\alpha(T)}$ obtained by setting $\sum_{\Delta h}|x^{\alpha}_{\Delta h}(T)|^2=1$ is

$$N^{L_T}_{\alpha(T)}=\left\{(4/3)^2(1/4\pi)\times\sum_{n_\Delta l_\Delta n_h l_h}\left[R^{\Delta h}_{L_T}\hat{l}_\Delta\hat{l}_h\begin{bmatrix}l_\Delta & L_T & l_h\\ 0 & 0 & 0\end{bmatrix}\right]^2\right\}^{-1/2} \tag{3}$$

and the Δ-hole matrix element $O^{J_TL_T}_{\Delta h}$ is

$$O^{J_TL_T}_{\Delta h}=(4/\sqrt{3})(-1)^{(l_h+L_T+1)}R^{\Delta h}_{L_T}\hat{l}_\Delta\hat{l}_T\hat{l}_h(4\pi)^{-1/2}\begin{bmatrix}l_\Delta & L_T & l_h\\ 0 & 0 & 0\end{bmatrix}\hat{j}_\Delta\hat{j}_h\begin{Bmatrix}l_h & l_\Delta & L_T\\ 1/2 & 3/2 & 1\\ j_h & j_\Delta & J_T\end{Bmatrix}. \tag{4}$$

The Δ-hole matrix element, then, is proportional to the 9-j symbol as a result of coupling the Δ-hole states microscopically, as well as coupling the overall nuclear states such that $J_T=L_T$, $L_T\pm1$. The large Δ-hole radial integral is

$$R^{\Delta h}_{L_T}=\int_0^\infty d\xi u_{n_\Delta l_\Delta}(\xi)\xi^{L_T}u_{n_h l_h}(\xi)$$

which contains the radial shell-model states. Because of

degeneracy, the sums in (3) are only over the principal and orbital angular momentum quantum numbers. The caret symbolizes $\hat{j}=\sqrt{2j+1}$. Similar expressions are obtained for the particle-hole coefficients for the projectile. After these coefficients are substituted into the nuclear form factors described in [8], and for fixed multipole values (J_T, L_T), the form factors become proportional to a sum of particle-hole states. The sums over j_Δ, j_h disappear because of the assumption of degeneracy which allows for the orthonormality property of the 9-j symbols to be taken over those values thereby simplifying the form factors. Again, the target form factors become proportional to the sum.

$$S_{L_T}(k)=N_{\alpha(T)}^{L_T}\sum_{n_\Delta l_\Delta n_h l_h}\left[\hat{l}_\Delta\hat{l}_h\begin{bmatrix} l_\Delta & L_T & l_h \\ 0 & 0 & 0\end{bmatrix}\right]^2 R_{L_T}^{\Delta h}(k)R_{L_T}^{\Delta h}, \tag{5}$$

where

$$R_{L_T}^{\Delta h}(k)=\int_0^\infty d\xi\, u_{n_\Delta l_\Delta}(\xi)j_{L_T}(k\xi)u_{n_h l_h}(\xi)\ .$$

It is interesting to note that the sum $S_{L_T}(k)$ becomes a coherent addition of degenerate Δ-hole states in the limit $k\to 0$. For the formation factor, k equals the projectile momentum transfer K, and, in the decay factor, k equals the pion wave number k_π. Again, a similar expression is obtained for the projectile form factor. In the calculations presented here, only the spin-isospin modes are excited so that $L_T=L_P=0$ and $J_T=J_P=1$. Finally, solving for the three-body, final-state phase space and kinematics, the pion differential cross section $d^3\sigma/d(p_\pi c)d\Omega_\pi d\Omega_p$ is obtained.

Also, I have extended this approach by including the central and tensor ρ-exchange terms in the microscopic interaction between nucleons. The model used for the π- and ρ-exchange transition interactions was obtained from Machleidt [11] and is more general than that used by Jain and Santra [12] since Machleidt's model includes the mass difference between the nucleon and isobar, and contains an additional combination of spin-orbit and transverse terms. In this work, the combination of terms [see (B.4) in Ref. [11] was neglected, since the coupling constants involved in this combination are almost an order of magnitude smaller than the coupling constants involved in the first term.

The questions of nuclear distorted waves and pion distortion and absorption are important, but will be explained and reported in the future. It is estimated that it would take several years to complete the work of introducing these effects into the calculation and generating the necessary codes that would carry out the calculations. The present formalism is itself long and complicated and took a sizable period of time to complete. It is felt that there is quite a bit of physics to be learned at the present stage such as nuclear structure effects, effects of the central versus tensor terms in the nucleon-nucleon interactions, energy-dependent effects, and phase-space considerations before the complications of distortion and absorption are included. The calculations at their present stage are necessary and have to be done first so that the questions of how sensitive and in what way does distortion and absorption affect the results can be answered. Because of the immediacy and interest in the role that coherence might play in these reactions, it is felt that the present theoretical results will serve as a useful indicator and motivator for future experiments.

In order to carry out comparative calculations of the pion-differential cross sections on C+C, typical target Δ-hole states were chosen for the sums in Eqs. (3) and (5) and were then used as a common basis in order to compare the pion energy distributions for different incoming projectile energies. Since spin-flip mechanisms are the ones under study, the $(1p_\Delta)(1p)^{-1}$ states were chosen in the valence shell. Also, the core states $(1s_\Delta)(1s)^{-1}$ were included since no absorption was assumed and it would allow for maximal pion production. The calculations also contain higher-order contributions from the $(2p_\Delta)(1p)^{-1}$ and $(2s_\Delta)(1s)^{-1}$ states; however, these contributions are small and do not appreciably change the shapes or magnitudes of the energy distributions from the lowest-order contributions. The particle-hole states chosen for the projectile $M1$ excited state at 15.11 MeV of ^{12}C were the usual $(1p)(1p)^{-1}$ states. A more detailed investigation of the shell-model effects on the pion distributions will be described in a subsequent paper since the purpose here is

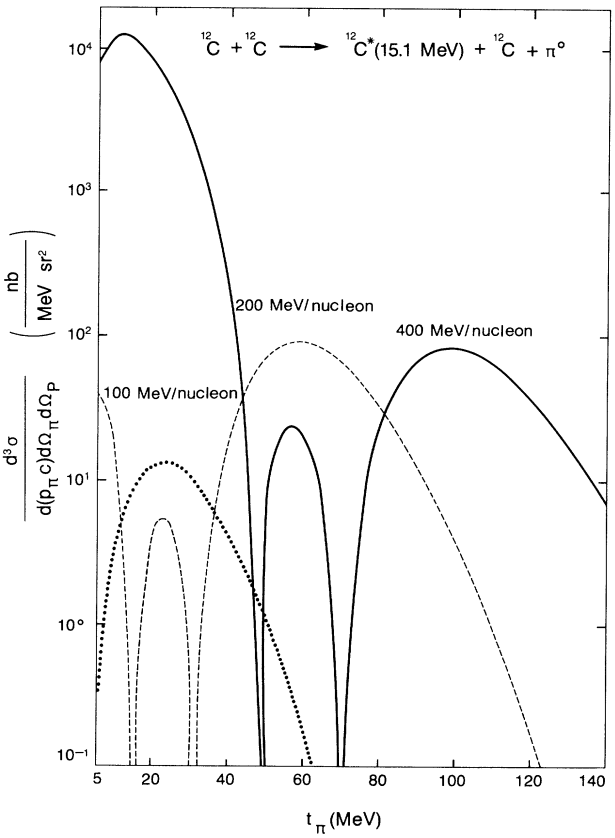

FIG. 1. Theoretical π^0 production at 100 MeV/nucleon (dotted curve), 200 MeV/nucleon (dashed curve), and 400 MeV/nucleon (full curve) incident energies calculated at forward projectile and pion angles in the nucleus-nucleus, center-of-mass frame.

to see how the distributions change as the incident energies are increased.

The results of the pion kinetic energy distributions are shown in Fig. 1 for incident projectile energies of 100 MeV/nucleon (dotted curve), 200 MeV/nucleon (dashed curve), and 400 MeV/nucleon (full curve). Because the formation and decay amplitudes are proportional to spherical harmonics [see Eqs. (13) and (20) in Ref. [8]], forward angles for the projectile ($\theta_P = 0°$) and pion ($\theta_\pi = 0°$) were chosen since the angular dependence is maximized. Also, because of the forward angle condition, the ρ-exchange amplitude gives no contribution due to angular coupling properties in the formation amplitudes. The curves shown are then a direct reflection of the π-exchange effects only. The interesting result of these distributions is the appearance of more structure when the incident energy increases. At 100 MeV/nucleon, there is a single lobe which maximizes near 23 MeV; at 200 MeV/nucleon, a small secondary lobe appears with the beginnings of a primary lobe appearing at low energies; and at 400 MeV/nucleon, there are primary, secondary, and tertiary lobes appearing with the primary lobe showing itself more fully. These structures appear because the formation amplitude has three lobes as a function of projectile momentum transfer K. The lobes in the distributions seem to "walk" to the right from low to high incident projectile energy because, for a given value of pion kinetic energy t_π, the values of K decrease with increasing projectile energy, which is a consequence of the three-body kinematics in the final state. Higher projectile energies suffer less momentum transfer for fixed t_π. At 100 MeV/nucleon, the dotted curve in Fig. 1 reflects only the tail of the formation amplitude which has a tertiary maximum at the K values sampled. At 200 MeV/nucleon, the range of K values moves towards smaller values, and encompasses a secondary maximum found between two zeros. The structure seen in the dashed curve reflects these two lobes for the K values sampled. At 400 MeV/nucleon, the K values drop even further and encompass all three lobes found in the formation amplitude for the range of pion kinetic energies shown in Fig. 1. A calculation was also done at 800 MeV/nucleon and again a three-lobe structure appears which shifts to the right of the 400 MeV/nucleon curve. Therefore, the general feature from these calculations shows that for increasing incident energy, a three-lobe structure "walks" to the right where parts or all of this structure may be revealed depending on the range of K values allowed. These values themselves depend on the range of pion kinetic energies t_π given by the three-body kinematics in the final state. It should be pointed out that the energy dependence of the delta width has been included in these calculations; however, the resonance effect is not as pronounced as one might expect. In fact, the already broad energy-dependent delta width flattens out further as the pion distributions proceed to higher energies, and calculations of the resonance effect alone show that the shape is quite flat. This resonance is further flattened when the distributions are plotted semilogarithmically. Finally, the zeros in these distributions are symptomatic of a Born approximation calculation which overemphasizes structure, and it is expected that the zeros will be partially filled in when distortion is included. Furthermore, since these calculations are absorption free, the results represent a best case scenario, since absorption will dampen the values or the cross sections. However, these calculations show general structural features of the pion energy distributions and may provide a unique signature for this coherent process.

I gratefully thank my colleague W. Daniel Edwards for all his help and advice in the computational phase of this problem. I acknowledge the support of National Science Foundation Grant No. PHY-89-11040.

[1] B. Erazmus *et al.*, Phys. Rev. C **44**, 1212 (1991).
[2] D. Vasak, B. Müller, and W. Greiner, Phys. Scr. **22**, 25 (1980); D. Vasak, H, Stöcker, B. Müller, and W. Greiner, Phys. Lett. **93B**, 243 (1980); M. Uhlig, A. Schäfer, and D. Vasak, Z. Phys. A **319**, 319 (1984); D. Vasak, W. Greiner, B. Müller, T. Stahl, and M. Uhlig, Nucl. Phys. **A428**, 291c (1984); D. Vasak, B. Müller, and W. Greiner, J. Phys. G **11**, 1309 (1985).
[3] M. Tohyama, R. Kaps, D. Masak, and V. Mosel, Phys. Lett. **136B**, 2266 (1984); Nucl. Phys. **A437**, 739 (1985).
[4] A. Blin, C. Guet, and B. Hiller, GANIL Report No. P. 85/11, 1985.
[5] M. Prakash, C. Guet, and G. E. Brown, Nucl. Phys. **A447**, 625c (1985).
[6] C. Guet, M. Soyeur, J. Bowlin, and G. E. Brown, Nucl. Phys. **A495**, 558 (1989).
[7] P. A. Deutchman, R.L. Buvel, Khin Maung Maung, and J. W. Norbury, Phys. Rev. C **33**, 396 (1986); P. A. Deutchman and Khin Maung Maung, *ibid.* **41**, R423 (1990).
[8] P. A. Deutchman, Phys. Rev. C **45**, 357 (1992).
[9] P. Braun-Munzinger and J. Stachel, Annu. Rev. Nucl. Part. Sci. **37**, 97 (1987).
[10] J. M. Eisenberg and W. Greiner, *Microscopic Theory of the Nucleus* (North-Holland, Amsterdam, 1972), Vol. III, p. 200; D. J. Rowe, *Nuclear Collective Motion* (Methuen, London, 1970), p. 218; G. E. Brown, J. A. Evans, and D. J. Thouless, Nucl. Phys. **24**, 1 (1961).
[11] R. Machleidt, Adv. Nucl. Phys. **19**, 189 (1989); **19**, 354 (1989).
[12] B. K. Jain and A. B. Santra, Nucl. Phys. **A500**, 681 (1989).